Vaults. III. Vault Ribonucleoprotein Particles Open into Flower-like Structures with Octagonal Symmetry

Nancy L. Kedersha,* John E. Heuser,‡ Diane C. Chugani§ and Leonard H. Rome*

*Department of Biological Chemistry and the Mental Retardation Research Center, University of California at Los Angeles School of Medicine, Los Angeles, California 90024-1737; ‡Department of Cell Biology and Physiology, Washington University, St. Louis, Missouri 63110; and §Department of Radiological Sciences, Division of Nuclear Medicine, University of California at Los Angeles School of Medicine, Los Angeles, California 90024-1721

Abstract. The structure of rat liver vault ribonucleoprotein particles was examined using several different staining techniques in conjunction with EM and digestion with hydrolytic enzymes. Quantitative scanning transmission EM demonstrates that each vault particle has a total mass of 12.9 ± 1 MD and contains two centers of mass, suggesting that each vault particle is a dimer. Freeze-etch reveals that each vault opens into delicate flower-like structures, in which eight rectangular petals are joined to a central ring, each by a thin hook. Vaults examined by negative stain and conventional transmission EM (CTEM) also reveal the

flower-like structure. Trypsin treatment of vaults resulted exclusively in cleavage of the major vault protein (p104) and concurrently alters their structure as revealed by negative stain/CTEM, consistent with a localization of p104 to the flower petals.

We propose a structural model that predicts the stoichiometry of vault proteins and RNA, defines vault dimer–monomer interactions, and describes two possible modes for unfolding of vaults into flowers. These highly dynamic structural variations are likely to play a role in vault function.

A number of different ribonucleoprotein particles (RNPs)[1] have been identified in eukaryotic cells (Dreyfuss, 1986). Those particles whose functions are known are generally involved in RNA processing or translation. The larger RNPs have been examined by EM and in some cases morphological studies have provided important structural information. The ribosome has been closely examined by a number of high-resolution microscopic techniques including scanning transmission EM (STEM) (Boublik et al., 1982; Mandiyan et al., 1989) and negative staining and conventional transmission electron microscopy (CTEM) both with and without site specific antibodies (Wittmann, 1983). A detailed model of the ribosome has evolved that in many ways relates structure and function (Nierhaus et al., 1987). Signal recognition particle has been examined by CTEM and by STEM (Andrews et al., 1987) and a structural model has been proposed that relates its long rod-like shape with its proposed functions (Walter and Blobel, 1983; Siegel and Walter, 1988). Although less well-characterized than the previously mentioned examples, the spliceosome, a complex

macromolecular assembly that includes several small nuclear RNPs (snRNPs), has also been examined by CTEM (Busch et al., 1982; Reed et al., 1988). Structure–function insights have also been obtained using CTEM and STEM on other large macromolecular assemblies, notably nuclear pore complexes (NPCs) (Akey and Goldfarb, 1989; Akey, 1989; Reichelt et al., 1990) and clathrin-coated vesicles (Heuser, 1980; Crowther et al., 1976; Vigers et al., 1986; Steven et al., 1983).

Vaults are large cytoplasmic RNPs of unknown function, possessing a very characteristic morphology (Kedersha and Rome, 1986a) which is conserved among eukaryotes as diverse as rat and *Dictyostelium* (Kedersha et al., 1990). Negatively stained CTEM images of vaults revealed their dimensions to be 35 × 65 nm, considerably larger that ribosomes. As vaults from all species display similar size, composition, morphology, and immunologically similar protein composition, it is likely that vault structure is important to vault function.

Despite their large size, vaults are composed predominantly of a single polypeptide of M_r 104,000 (p104), which has been shown to constitute >70% of the total particle mass. Rat vaults were also shown to contain minimally 55 copies of p104 and 9 copies of the vault RNA; however, twofold symmetry considerations suggested these values might reflect only half the mass of an intact vault (Kedersha and Rome, 1986a). Such a high-copy multisubunit composition

1. *Abbreviations used in this paper:* CTEM, conventional transmission EM; NPC, nuclear pore complex; RNP, ribonucleoprotein particle; STEM, scanning transmission EM.

is unlike that of other RNPs, and is more typical of cytoskeletal elements, coated vesicles, and viruses. Such structures are highly symmetrical, usually capable of self-assembly and disassembly under physiological conditions, and often perform mechanical and structural functions. By analogy, vault structure and composition suggest that its function may involve structural/mechanical aspects.

The methods of imaging employed in this study reveal that vault structure is indeed highly ordered and quite complex. We propose a structural model that predicts the absolute stoichiometry of the major vault protein and the vault RNA, and suggests that vaults may be capable of major conformational rearrangements in vivo.

Materials and Methods

Vault Purification

Vaults from rat liver were purified essentially as described previously (Kedersha and Rome, 1986a,b). In most recent preparations, 1.0 mM DTT has been included throughout all stages of purification in order to prevent oxidation.

EM

STEM was performed by Drs. James F. Hainfield, Joseph Wall, and Paul S. Furcinitti at the Brookhaven National Laboratory on rat vault samples previously dialyzed against 10 mM ammonium acetate. Tobacco mosaic virus was included as an internal calibration standard. Negatively stained specimens were prepared using 1% uranyl acetate and carbon-coated grids. Freeze-etch analysis of vaults was performed on vaults absorbed to polylysine-treated mica before quick-freeze and freeze-fracture as described elsewhere (Heuser 1983; Heuser and Goodenough, 1984; Heuser and Kirchausen, 1985). Frozen hydrated specimens were prepared by Drs. Timothy Baker and Norman Olson of Purdue University (Olson and Baker, 1989).

Crystalline arrays of vaults were obtained by mixing purified vaults (at a concentration of ~500 μg/ml) with 9 vol of 1% cytochrome C or 1% polylysine in MES buffer. Samples were allowed to adsorb to carbon-coated grids for 1-2 min at room temperature, and excess sample was removed by gentle blotting with filter paper. The grid was then stained by immersion in 1% uranyl acetate that contained a second carbon film floating on the surface. This second film was picked up onto the sample-coated grid, creating a carbon sandwich around the stained particles. The sandwich was air dried for 1 min before blot/drying on filter paper (Whatman Inc., Clifton, NJ). Conventional negative staining was performed by adsorbing vault particles onto carbon-coated grids for 1-2 min, blotting off the sample, and adding 1% uranyl acetate for 30 s to 1 min. Excess stain was then removed by blotting and the specimen air-dried.

Other Procedures

Vaults were treated with trypsin using a 10:1 ratio (wt/wt) of vault protein to trypsin, in 50 mM MES buffer, pH 6.5, for 2 h at room temperature. These conditions allow the complete cleavage of p104 without affecting the other vault polypeptides or the vault RNA. The reaction was terminated with soybean trypsin inhibitor, and the vault protein separated from trypsin and the inhibitor by sedimentation through sucrose in a airfuge (Beckman Instruments, Inc., Palo Alto, CA). Proteins were resolved on SDS-PAGE,
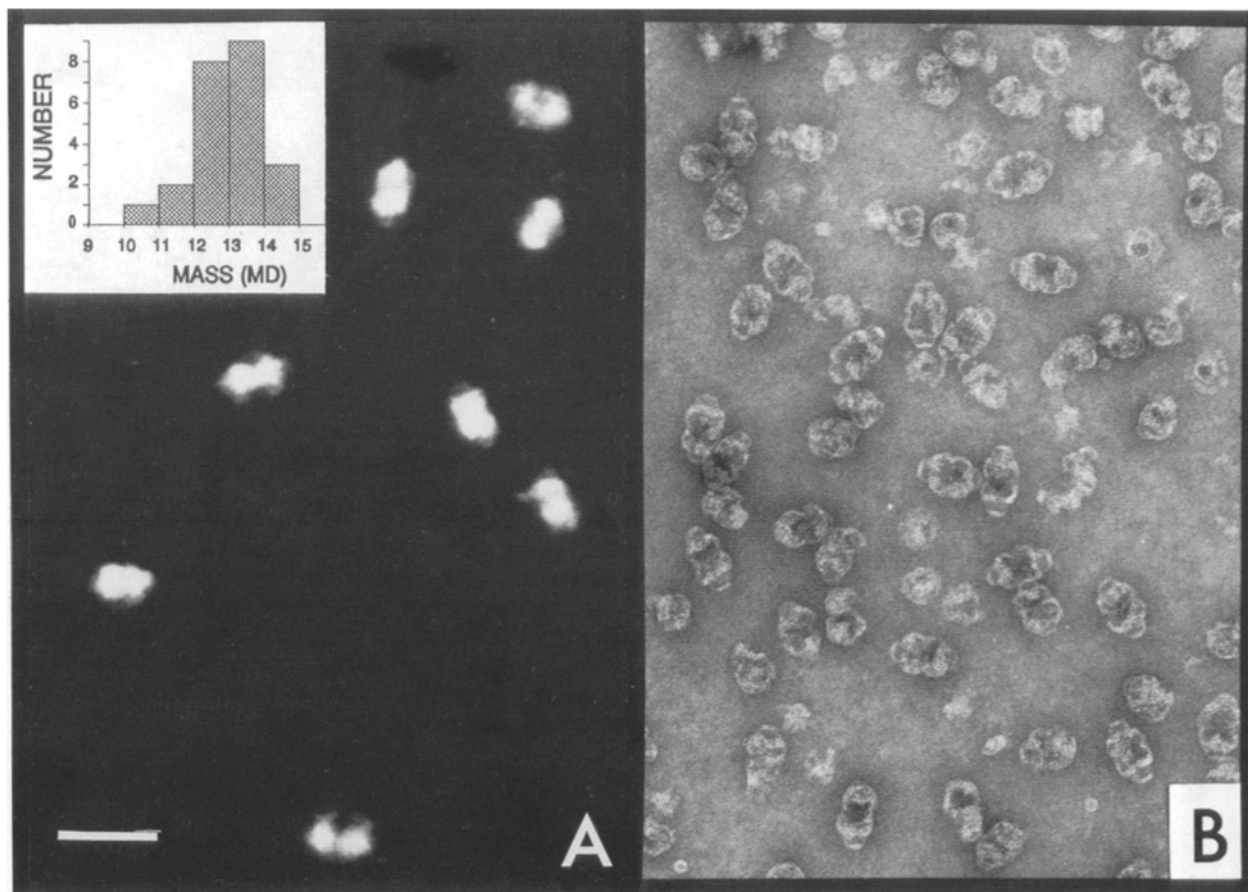

Figure 1. Rat liver vaults viewed by different techniques. (*A*) RNAase A–treated rat liver vaults viewed by STEM. Tobacco mosaic virus was used as an internal standard but is not shown in this field. (*inset*) Mass distribution of RNAase-treated vaults viewed by STEM. (*B*) Rat liver vaults stained with uranyl acetate. Bar, 100 nm.
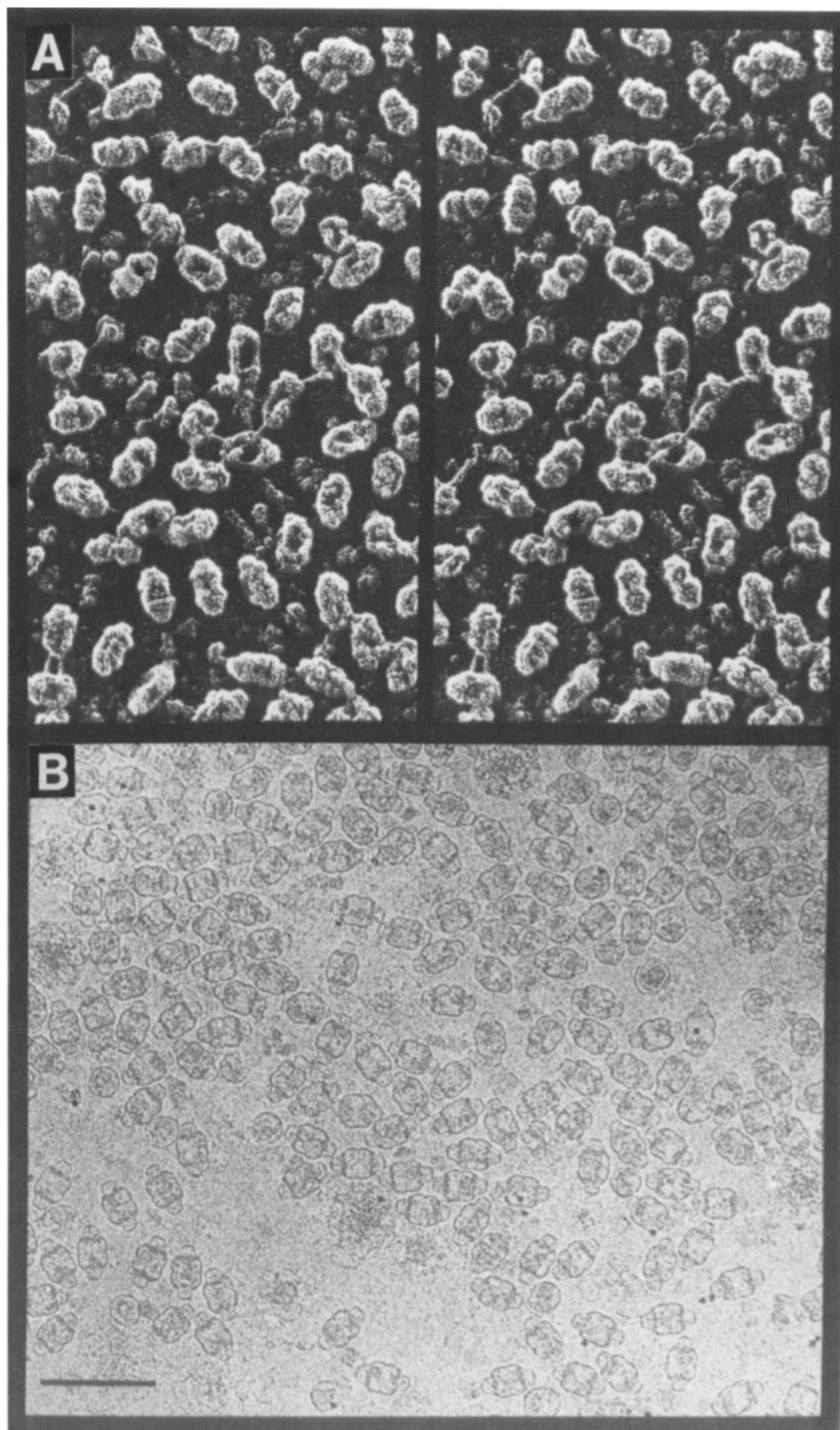
Figure 2. Rat liver vaults viewed by different techniques. (*A*) Stereo images of rat liver vaults subjected to freeze-etch and rotary shadowing. Note that many vaults appear hollow when viewed using stereo glasses. (*B*) Frozen hydrated vaults viewed by cryoelectron microscopy. Bar, 100 nm.

stained with Coomassie brilliant blue R, and scanned using an ultrascan XL laser densitometer (LKB Instruments, Inc., Gaithersburg, MD). Stoichiometric relationships between the vault proteins were determined using the apparent molecular weights to convert integrator values to moles, and molar ratios determined accordingly.

Results

Vault Mass Determination by STEM

When rat liver vaults were examined by STEM, oblong

Table I. Dimensions of Rat Liver Vaults Obtained Using Different EM Techniques

	Length	Width	l/w	N
	nm	*nm*		
Negative stain	61.8	34.0	1.82	65
Freeze-etch	56.7	32.3	1.76	42
Frozen-hydrated	48.7	26.4	1.84	53
STEM	59.4	34.8	1.71	23

structures were observed that possessed a twofold symmetry containing two distinct and apparently equal centers of mass. The best STEM images obtained were of vaults that had been previously treated with RNAase A to digest vault RNA (Fig. 1 A). Samples not RNAase treated had an identical morphology and very similar mass (not shown). The structures revealed were similar to those seen using negative stain and CTEM (Fig. 1 B). Since the vault RNA appears to constitute <5% of the particle mass (Kedersha and Rome, 1986a), it is not surprising that the RNAase-treated samples were indistinguishable from native vaults as the expected reduction in mass would be less than the 8–10% error inherent in the technique. CTEM (negative stain) morphology and migration rate on agarose gels were likewise unaffected by the RNAase treatment (see below). The mass distribution of the RNAase-treated vaults is shown in Fig. 1 A (*inset*). The average mass value of a single vault was 12.9 ± 1 MD, using tobacco mosaic virus as an internal standard (Mosesson et al., 1981). This value is consistent with the sedimentation behavior of vault particles on velocity sucrose gradients

(∼150S), as they appear larger than ribosomes (the 80S ribosomal particle has a molecular mass of ∼3.6 MD) and smaller than most rat liver coated vesicles, which range in size from 150 to 300S (Prasad et al., 1984) and vary considerably in mass (Steven et al., 1983).

Cryoelectron and Freeze-Etch Microscopy

When purified rat liver vaults were subjected to rapid freezing followed by platinum shadowing (Heuser, 1983; Heuser and Kirchausen, 1985), structures were observed (Fig. 2 A) that were also similar in overall shape and size to negatively stained images (Fig. 1 B). The freeze-etch profiles revealed more of the three-dimensional shape of the particles and fewer of the internal contours that give negatively stained vaults their multiple arch-like appearance. The overall shape of the vault structure appears similar by both freeze-etch and negative stain, thus confirming that vault symmetry in not grossly altered by treatment with uranyl acetate. Freeze-etch stereo pairs revealed that vaults may be somewhat hollow (Fig. 2 A). Frozen-hydrated samples of vaults were also examined using cryoelectron microscopy, a technique which in many cases minimizes preparation artifacts (Olson and Baker, 1989). The images obtained (Fig. 2 B) by this technique show structures with greatest similarity in shape to those seen by negative stain (Fig. 1 B). A comparison of dimensions obtained using each technique is presented in Table I. The length/width ratios measured from images obtained using STEM and cryoelectron microscopy were in closest agreement, favoring a more rounded vault. Both freeze-etch and negative stain resulted in more ellipsoid
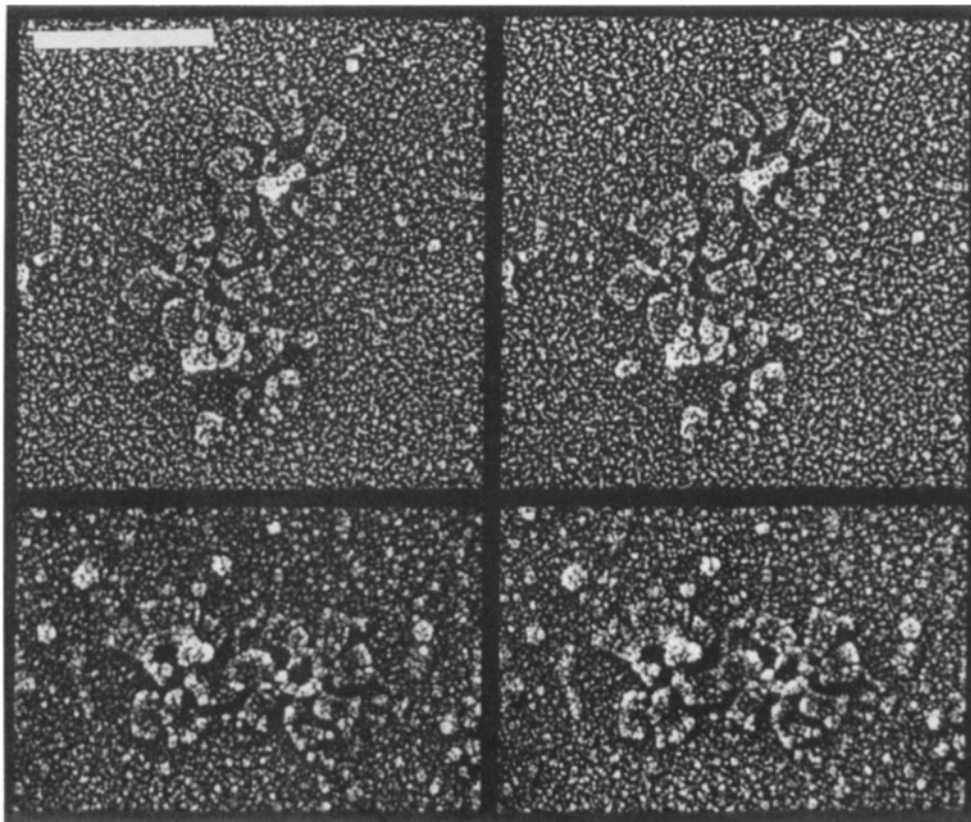

Figure 3. Fully opened vaults, showing the pair of flowers that derive from a single vault. Stereo paired images of open vault flowers revealed by freeze-etch, showing that each flower is composed of eight rectangular petals surrounding a central ring each connected to the ring by a short hook emanating from one corner. Bar, 100 nm.
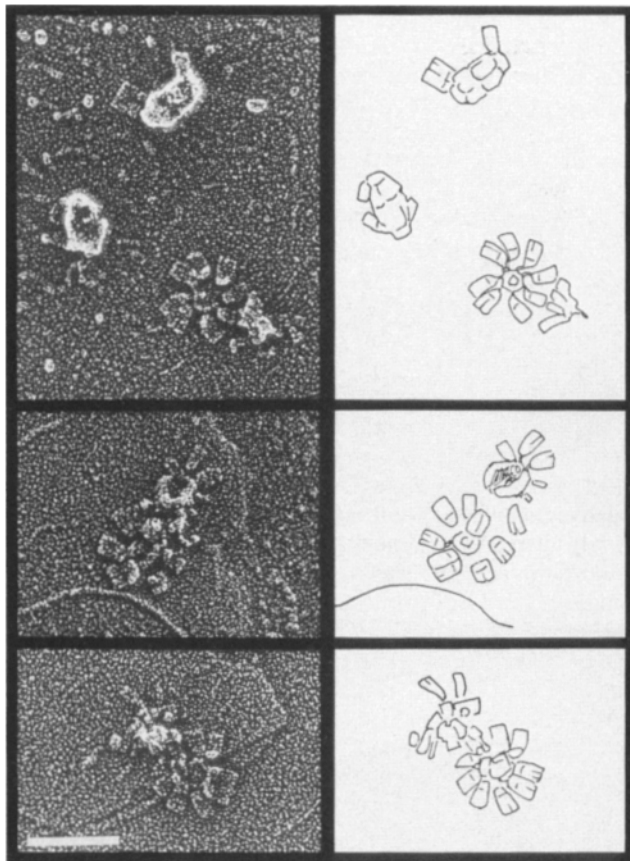
Figure 4. Vaults unfolding in vitro. Images of partially opened vaults, freeze-etch preparation, showing representative examples of vaults in various stages of unfolding. (*left panels*) Electron micrographs. (*right panels*), Artist's sketch. Bar, 100 nm.

morphology. Least in agreement were the absolute size measurements. The "truest" values relative to the in vivo situation are likely those obtained with cryoelectron microscopy, as it avoids the use stain or platinum shadowing altogether. In addition, vaults visualized by this technique were the most uniform in appearance, size, and dimensions.

The freeze-etch procedure also revealed a new and completely unexpected structural complexity. In many areas of the polylysine-coated mica, vaults "opened" into flower-like structures (Fig. 3). The flowers were usually seen in pairs, suggesting that an intact vault was comprised of two folded flowers. Upon close examination of numerous fields, each flower was composed of eight rectangular petals surrounding a central ring; the corner of each rectangular petal was connected to the ring by a thin, short hook. This stoichiometry was further supported by examination of partially opened vaults. A collage of such images is displayed in Figs. 4 and 5, along with accompanying interpretative sketches. Regular segments of the outer edges of the compact vault ovoid disappeared as the vault petals became exposed, suggesting that the petals are arranged evenly around the outside surface of the vaults in the intact structure. Further examination of opened vaults using both mono and stereo images revealed an additional fine structural detail: vault petals often appeared to be split lengthwise into three apparently equal seg-

ments, and occasionally into two equal or unequal segments (see Figs. 4 and 5).

A reexamination of negatively stained preparations also revealed the presence of flower-like structures (see Fig. 7 *C, lower panel*). These were difficult to see by negative stain except in areas where the stain was rather heavy. The border between individual petals was less defined in these images than those unfolded during freeze-etch. The number of flower-like structures seen by both freeze-etch and negative stain varied greatly in different areas of the same grid, suggesting that variable unfolding occurred during the specimen preparations. Several treatments were tried in conjunction with freeze-etch in order to facilitate vault unfolding. Brief treatment with high concentrations of NaCl (1.5 M), detergent treatment (1.0% NP-40), and treatment with 0.5% β-mercaptoethanol did not appreciably increase the frequency of opened structures (data not shown).
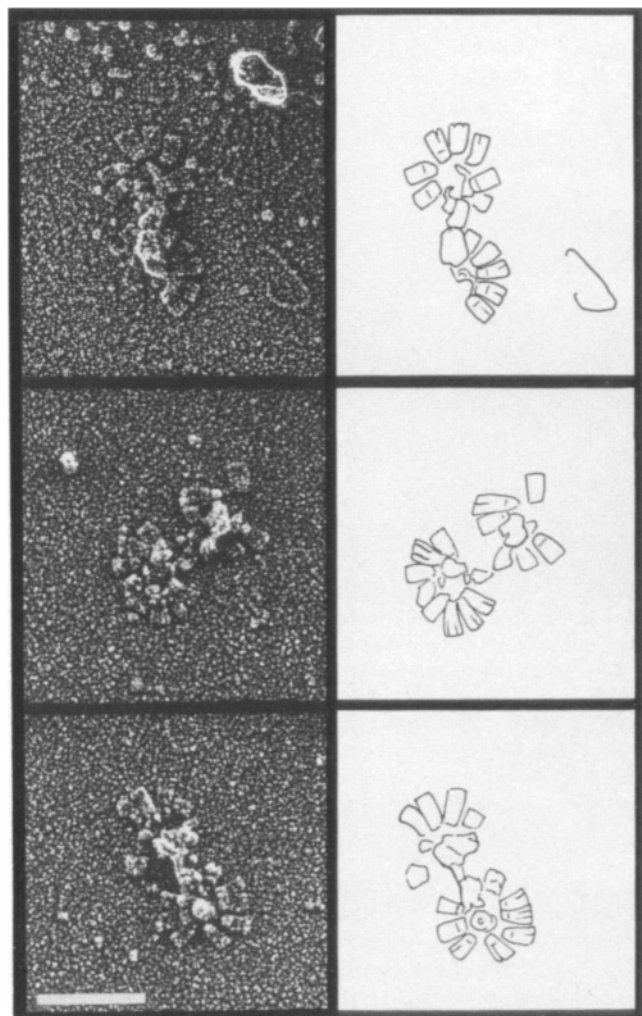

Figure 5. Vaults unfolded in vitro. Images of vaults in the later stages of opening, revealing the paired flowers. (*left panels*) Electron micrographs. (*right panels*) Artist's sketch. Note the tendency of the individual petals to split lengthwise into two or three parts. Bar, 100 nm.
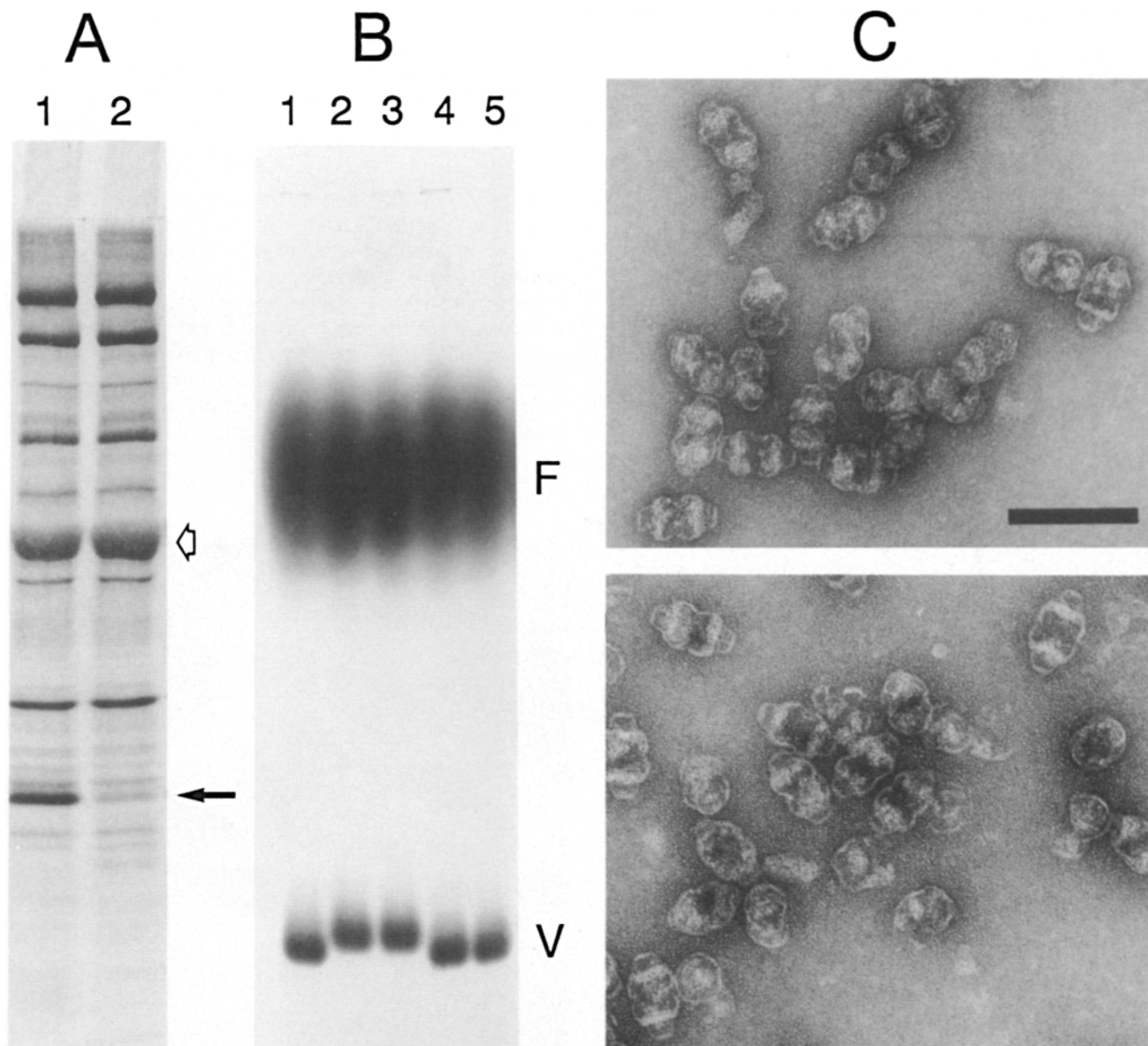
Figure 6. Rat liver vaults treated with ribonuclease A or trypsin. (*A*) Rat vaults (1 µg) in MES buffer were incubated for 2 h at room temperature either without (lane *1*) or with (lane *2*) 500 ng RNAase A, then resolved on an 8/12% step acrylamide gel in SDS (see Kedersha and Rome, 1986*a*) and visualized with silver stain. The RNAase completely removed the RNA (*solid arrow*); the small band remaining after RNAase treatment stains with Coomassie (not shown) and is therefore protein. The migration position of p104 is indicated by the open arrow. (*B*) Rat vaults and ferritin were treated with RNAase as described above (lanes *3* and *4*) or trypsin as described in the legend to Fig. 6 (lanes *2* and *3*) and subjected to electrophoresis on a 0.4% agarose gel in 50 mM MES, pH 6.5. Only trypsin treatment (lanes *2* and *3*) altered the mobility of the vaults (lower bands, designated with the letter *V*), the mobility of ferritin (*F*) was unaffected. (*C*) Electron micrographs of negatively stained untreated (*top*) and RNAase-digested (*bottom*) rat liver vaults. Bar, 100 nm.

Effect of RNAase A and Trypsin on Vault Structure

As the vault RNA comprises <5% of the total mass of the vault particle (Kedersha and Rome, 1986*a*), a structural role for the vault RNA seemed unlikely. To test this possibility, we removed the RNA from intact rat liver vaults by digestion with RNAase A and confirmed that the RNA was completely removed by analysis on SDS-PAGE (Fig. 6 *A*). The RNAase-treated vaults exhibited no change in mobility on sucrose gradients (not shown); however, given the small mass contribution of the RNA to the total particle this method was not sufficiently sensitive to determine definitively whether an alteration in the structure of the vault particles occurred.

Agarose gel electrophoresis under native conditions was also employed since this method is able to detect slight structural changes. No change in mobility of the RNAase-treated vaults was noted under conditions that could detect structural changes that result from trypsin treatment (Fig. 6 *B*, compare lanes *4* and *5* [RNAase A treated] with lanes *2* and *3* [trypsin treated] versus lane *1* [control]). Finally, CTEM of RNAase-treated vaults (Fig. 6 *C, bottom*) revealed no differences in vault structure as compared to untreated control vaults (Fig. 6 *C, top*). From this we conclude that the RNA is not a structural component of mature vaults analogous to that proposed for the 7SL RNA in signal recognition particle (Siegel and Walter, 1988; Andrews et al., 1987). The possibility of a role
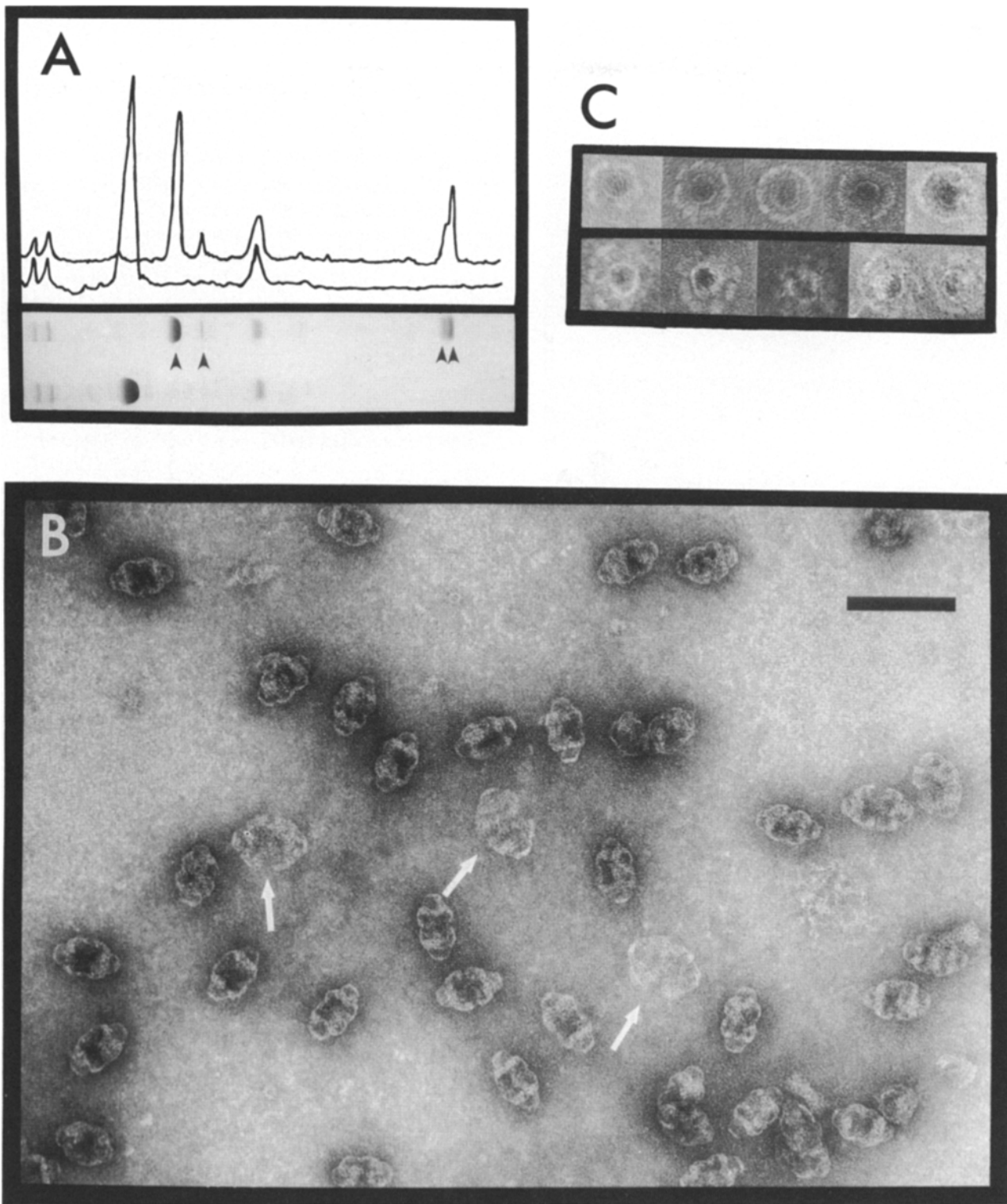
Figure 7. Trypsin treatment only digests p104, which largely affects vault radial stability. (*A*) Native vaults were treated with trypsin and sedimented through 30% sucrose in a Beckman airfuge. The pellets and supernatants were then treated with SDS and resolved on a 10% polyacrylamide gel and stained with Coomassie blue R. (*top lane and upper densitometer tracing*) Tryptic digest; (*bottom lane and lower densitometer tracing*) native vaults. The p104 is completely cleaved into four major fragments (indicated by *arrowheads*), while the other vault polypeptides are unaffected. All the polypeptides sediment as a large particle; the supernatant lanes were blank (not shown). (*B*) Field of vaults digested with trypsin. Many vaults appear unaffected, but several (*arrows*) have collapsed on their sides as a result of the trypsin treatment. (*C*) End views of negatively stained half vaults, showing the slight reduction in diameter as a result of trypsin digestion (*upper row*) as compared to native vaults (*lower row*). *C* is shown at 40% greater magnification than *B*. Bar, 100 nm.
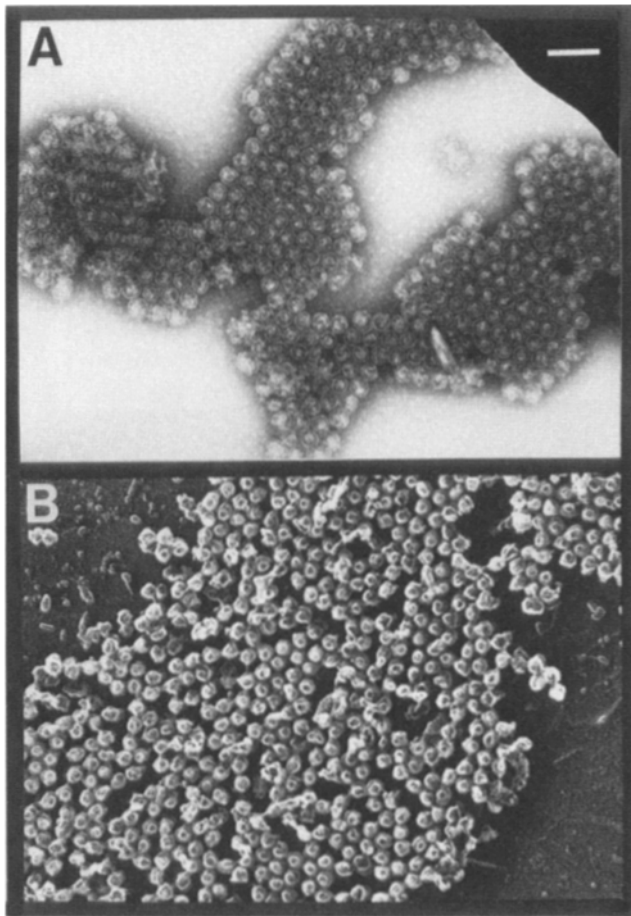
Figure 8. Vaults form pseudocrystalline arrays. (*A*) Vaults were mixed with cytochrome C and prepared using the carbon sandwich technique as described in the text. (*B*) Vaults spontaneously aggregated on polylysine-coated mica before freeze etch. Bar, 100 nm.

of the vault RNA in biosynthetic assembly of the vault particle cannot be ruled out.

Trypsin treatment of vaults resulted exclusively in cleavage of p104 into four major fragments of M_r ∼75,000, 70,000, 35,000, and 32,000 (Fig. 7 *A*). Complete tryptic cleavage of the p104 did not seem to affect the size of the whole vault particle as determined by velocity sucrose gradients (not shown), although it did reduce the mobility of vaults in native agarose gels (Fig. 6 *B*, lanes 2 and 3). When trypsin-treated vaults were negatively stained with uranyl acetate and examined by CTEM, two major differences in vault structure were observed. Vaults lying on their sides were frequently flattened and collapsed onto the carbon support, suggesting that cleavage of the p104 resulted in loss of radial integrity (Fig. 7 *B*, arrows), consistent with a radial localization of p104 in the intact vault structure. Less frequently observed were the flower-like structures mentioned above (Fig. 7 *C*). In the trypsin-treated sample these structures appeared to be smaller, possibly representing single flowers with trimmed petals. They were only seen in negatively stained preparations and could not be seen by the gentler procedure of freeze-etch. Rings possessing more defined petal-like outer edges were seen in untreated vaults (Fig. 7 *C*, lower panel), compared to trypsinized vault preparations, in which the

outer edges formed a more uniform halo (Fig. 7 *C*, upper panel). Thus, both structural changes observed in trypsin-treated vaults (flattening and loss of petal detail) are consistent with a radial localization of the petals, comprised of p104.

Polycations Induce Vault Crystals In Vitro

In an attempt to generate more "open" vaults to view by negative stain, we hypothesized that the polylysine used in conjunction with the freeze-etch technique might facilitate vault unfolding. We therefore mixed vaults with polylysine or cytochrome C (pI 10.6) before adsorption onto carbon films and negative stain. Vaults were frequently observed to aggregate under these conditions (not shown). Polycation treatment in conjunction with the double-sandwich carbon technique (Lake, 1978) yielded large pseudocrystalline arrays, in which vaults appeared to aggregate side-to-side, forming planar hexagonal lattices. Both polylysine and cytochrome C facilitated the formation of these structures; those induced by cytochrome C possessed more linear edges (Fig. 8 *A*). Occasional aggregates were also observed by freeze-etch (Fig. 8 *B*); however, these were less compacted and less regular. These results suggest that the sides of vaults are negatively charged. While the biological significance of these vault arrays is unclear, we were able to accurately confirm our earlier width estimates by measuring long runs of packed vaults and dividing by the number of particles present. Measurements obtained in this manner indicate that the diameter of a single vault is 36.1 nm, in good agreement with our earlier value of 35 nm obtained on negatively stained specimens (Kedersha and Rome, 1986a).

Discussion

A Model of Vault Structure

From the images obtained using a variety of EM techniques, we propose a model of vault structure (Fig. 9). Each vault comprises a hollow, barrel-like structure, composed of two identical cup-like halves joined at their open ends (Fig. 9). Each half vault is in turn composed of a single eight-petaled flower, which is folded into the cup shape. Each plate-like petal may be split lengthwise into two or three roughly equal parts.

The petals, as revealed by freeze-etch, comprise the bulk of the vault mass as does the p104 protein; it therefore seems likely that the petals are largely composed of p104. Furthermore, trypsin treatment only cleaves p104 (Fig. 7 *A*) and concurrently disrupts the radial integrity of the vault (Fig. 7 *B*), suggesting that intact p104 is required to maintain the barrel-like shape of the vault. In addition, end views of trypsinized vaults suggest that the petal is the major structure of the vaults that is affected by trypsin treatment (Fig. 7 *C*).

The model shows the petals folding into the vault particle with the underside of each petal facing outward in the intact vault. Folding intermediates shown by freeze-etch (Figs. 4 and 5) suggest that this is the case. In addition, vault unfolding into flowers on polylysine-treated mica suggests that the outer parts of the petals are negatively charged. The side-to-side aggregation of intact vaults into tightly packed pseudocrystalline arrays in the presence of soluble polycations
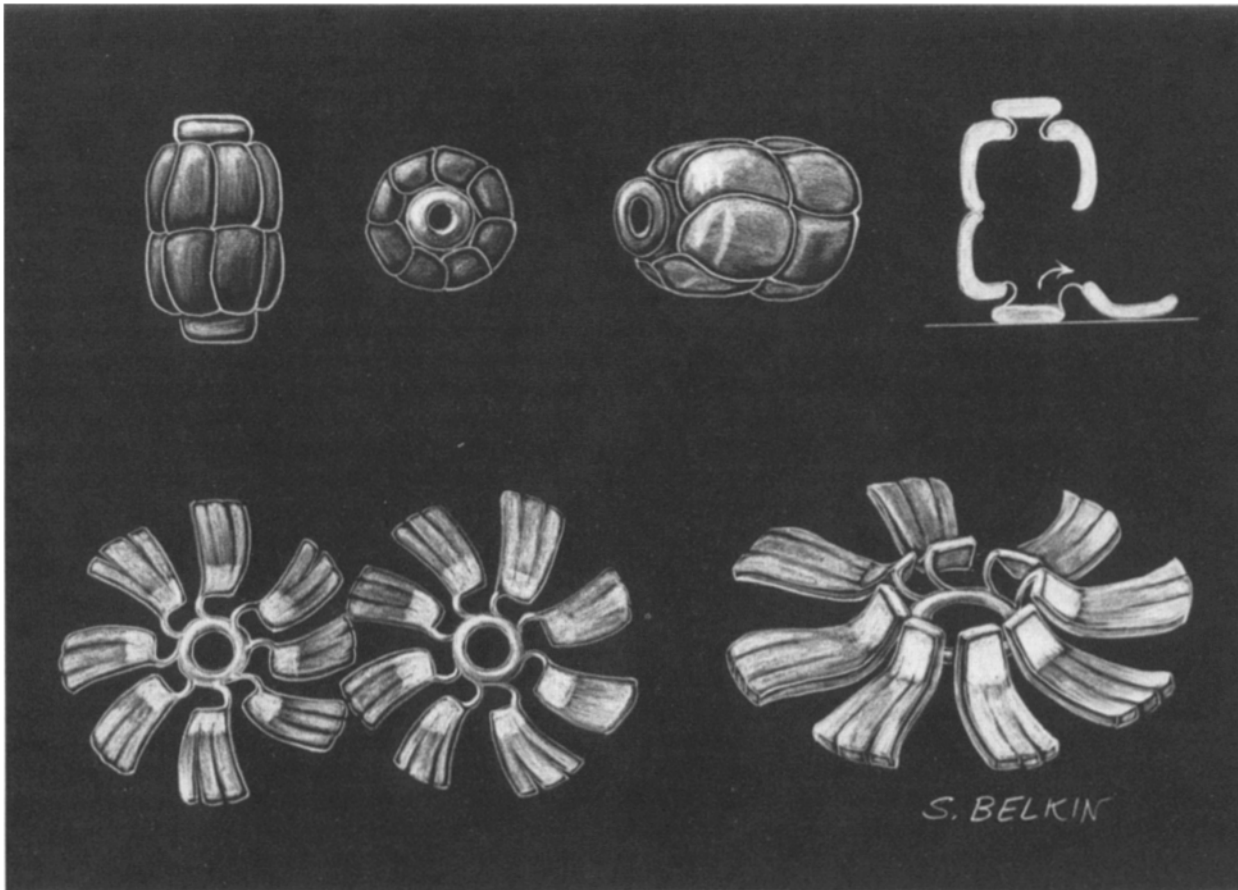
Figure 9. Model showing the folding of vault flowers into vaults. (*top row*) Side, end, and angled views of an intact vault, with a cross-sectional view showing one of two possible pathways leading to unfolding (see text). (*bottom row* Left) Paired vault flowers, derived from a single vault; (*bottom row, right*) three-dimensional rendering of a single vault flower viewed at an angle.

such as polylysine and cytochrome C (Fig. 8 *A*) also suggests that the outer sides of the vaults are negatively charged. Taken together, the data support a model of vault structure in which p104 constitutes all or most of each vault petal, which requires intact p104 for radial integrity of the intact vault, and is negatively charged on its outer radial surface.

Vaults can apparently separate into identical halves without unfolding into open flowers; such half vaults are occasionally observed in negatively stained preparations of vertebrate vaults but constitute the predominant form observed in vault preparations from *Dictyostelium* amebas (Kedersha et al., 1990). Whether half vaults open into flowers in vivo is unknown; however, the symmetry of the eight-petaled flowers is strikingly nonrandom and strongly suggestive of biomechanical function. Assuming that such an unfolding does indeed occur in vivo, two alternate models of opening are possible. In a two-step scenario, vaults dissociate into half-vaults before opening into flowers. In a one-step scenario as shown in our model (Fig. 9), vault unfolding may be coupled to dissociation into half-vaults, which might then constitute recycling intermediates en route to the reformation of whole vaults. Vaults are at least 10-fold more abundant in *Dictyostelium* than in vertebrate liver (N. Kedersha, unpublished observations), perhaps indicating that they are metabolically more important in *Dictyostelium*. The correlation

between abundance and prevalence of the half vault form could indicate that half-vaults are more likely to constitute the active form of vaults in this organism.

Previous stoichiometry measurements of the vault proteins suggested that vaults possess a minimum particle mass of 8 MD with each particle containing at least 55 copies of the major vault protein, p104. Symmetry considerations based on negatively stained images allowed us to speculate that the actual molecular mass of each vault might be twice that value (Kedersha and Rome, 1986*a*), and the data presented here confirm the notion that each vault is composed of two equal centers of mass. Assuming that p104 is found only in the petals, one can calculate the number of p104 polypeptides per vault using the following formula: Vmass $= 8 \times 2 \times N$ (104,000) $\times 1.33$, where 8 represents the number of petals per flower, 2 indicates that there are 2 flowers per vault, N indicates the number of p104 polypeptides per petal, and 1.33 corrects for the fact that p104 accounts for 74.6% of the total particle mass (this value was obtained using integrated peaks obtained from densitometer tracing shown in Fig. 7 *A*). Using integer values for N, Vmass values are obtained as follows: $N = 5$, Vmass $= 11.5$ MD; $N = 6$, Vmass $= 13.4$ MD; and $N = 7$, Vmass $= 15.6$ MD. The middle value of $N = 6$ gives the best agreement with the STEM mass estimate of 12.9 MD. Furthermore, since

each vault petal frequently appears split lengthwise into two or three equal parts (Figs. 4 and 5), assigning a value of six polypeptides per petal also provides an explanation of the observed symmetry.

While the location of the other peptides is a matter of speculation, it appears likely that p210, p192, and p54 comprise the central ring and connecting arms of the flower structures. The location of the vault RNA, which is not essential for the maintenance of vault structure by either freeze etch (not shown) or negative stain (Fig. 6 C), is similarly unknown. However, since the stoichiometry of the p104 to vault RNA was previously determined to be 6.4 to 1 (Kedersha and Rome, 1986a), it is likely that each petal (containing six molecules of p104) associates with one molecule of vault RNA.

Classification of Vaults by Structure

The extremely high copy number of p104 and the relatively large size of vault structures is reminiscent of clathrin-coated vesicles or cytoskeletal elements such as microtubules and actin stress fibers. These biological structures are capable of reversible self-assembly, and the in vivo state is characterized by a dynamic equilibrium between monomers, dimers (tubulin) or trimers (actin, clathrin triskelions), and much larger assemblies (microtubules, microfilaments). Less than 5% of the total vault p104 in cell extracts remains in the supernatant after centrifugation at 100,000 g for 1 h (N. Kedersha, unpublished observations), regardless of cell type (rat fibroblasts, Dictyostelium amebas) and using several different buffer systems. This suggests either that vaults do not exist in equilibrium with smaller soluble p104 complexes, or that the equilibrium greatly favors the assembled state. Vaults are not solubilized using 2 M urea, 1.0% Triton X-100, pH extremes from 4–10, ATP, or by several buffers (Pardee and Spudich, 1982) shown to depolymerize actin filaments (data not shown). This stability suggests that vaults may not disassemble into soluble components in vivo, but remain particulate once assembled. Rather than rearranging through cycles of polymerization and depolymerization, vaults may instead open and close like flowers.

High copy, multisubunit composition is also characteristic of viruses. However, the geometry revealed by the freeze-etch images indicates that vault structure is unlike that of known viruses although they are superficially similar in terms of size and multisubunit composition. Virus structures are broadly classified as either icosahedral or helical; the bacteriophages display both types of symmetry in their heads and tails. Vaults appear to consist of radially symmetrical flowers joined in a bilaterally symmetrical manner, unlike the icosahedral geometries of coated vesicles and viruses.

Possible Relationships between Vaults and NPCs

In terms of symmetry and geometry, the proposed vault structure is markedly similar to that of NPCs, in which eight-membered radial structures are paired within the outer and inner membranes of the nuclear envelope (Gall, 1967; Franke et al., 1981; Unwin and Milligan, 1982; Akey and Goldfarb, 1989; Akey, 1989; Reichelt et al., 1990). A series of models of the NPC have been proposed (Unwin and Milligan, 1982; Akey, 1989; Reichelt et al., 1990) based on ultrastructural studies employing EM methodology similar to that utilized here to examine vaults. The outer diameter of the NPC is ∼120 nm, slightly greater than that of open vault flowers seen by freeze-etch, which measure ∼100 nm. Therefore, open vaults and NPC are of similar but not identical diameter. One recent study (Reichelt et al., 1990) shows that the NPC "spokes" can be slightly bent, very much like the pinwheel arrangement of vault petals shown in Figs. 3–5. These striking similarities in both diameter and geometry suggest that vaults are somehow related to NPCs, possibly in terms of composition, function, or evolutionary lineage.

NPC polypeptides have been reported of M_r ∼210,000 (Snow et al., 1987), 190,000 (Gerace et al., 1982), 100,000 (Holt et al., 1987), and 54,000 (Snow et al., 1987); seemingly identical in mass to the major vault polypeptides of 210,000, 192,000, 104,000, and 54,000 (Kedersha and Rome, 1986a). All of these NPC polypeptides are glycosylated and many react with wheat germ agglutinin including those of M_r ∼210,000 and 54,000, due to the presence of O-linked N-acetylglucosamine residues (Snow et al., 1987; Holt et al., 1987; Hanover et al., 1987). No vault polypeptides react with wheat germ agglutinin (Kedersha and Rome, 1986a), however, the lack of detectable carbohydrate on vault polypeptides does not rule out the possibility that vaults constitute a pool of precursor NPC components or assembly intermediates that become glycosylated upon insertion into the nuclear membrane. Stoichiometric considerations argue against this possibility, as the major NPC polypeptides are present in approximately equimolar amounts, while the vault p104 constitutes 74.6% of the total vault protein. Cellular fractionation in conjunction with immunoblots and immunofluorescence indicates that most vault protein is present in readily extractable, cytoplasmic particles (Kedersha, N. L., D. C. Chugani, and L. H. Rome, unpublished observations), with a small (<5%) but reproducible amount of vault protein associating with the nuclear fraction. It would therefore appear that the bulk of vault protein is not associated with the nucleus and that vaults are unlikely to constitute components of mature NPCs.

A functional relationship between vaults and NPCs involving a physical interaction between the two, possibly a "docking" interaction between vaults and nuclear pores, could account for their structural similarities. Interestingly, the "central plug" of the NPC is a "roughly spherical" structure which appears to be removably associated with the NPC on the cytoplasmic face (Reichelt et al., 1990). The mass of this central plug has recently been determined by STEM to be 13 MD (Reichelt et al., 1990), identical to the mass of a vault. Furthermore, there is evidence that the plug itself displays 822 symmetry like NPCs and vaults (Akey, 1990). These central plugs are associated with only a subpopulation of NPCs in isolated nuclear membranes, suggesting that a minor fraction of the plugs may be associated with the nuclear envelope and that their steady-state distribution could be largely cytoplasmic. This raises the possibility that vaults constitute the plugs themselves. The docking of vaults/plugs at the NPC could involve some degree of vault unfolding, facilitated by vault petal/NPC spoke interactions. While such a possibility is highly speculative, immunofluorescence studies of isolated nuclei localize vaults to nuclear membranes (Chugani, D. C., N. L. Kedersha, and L. H. Rome, manuscript in preparation). A role for vaults in nuclear transport is consistent with the geometries of vaults and

NPCs, the cytoplasmic distribution of vaults, the abundance of vaults in oocytes, and the strong evolutionary conservation of structure displayed by both vaults and nuclear pores.

References

Akey, C. W. 1989. Interactions and structure of the nuclear pore complex revealed by cryoelectron microscopy. *J. Cell Biol.* 109:955–970.

Akey, C. W. 1990. Visualization of transport-related configurations of the nuclear pore transporter. *Biophys. J.* 58:341–355.

Akey, C. W., and D. S. Goldfarb. 1989. Protein import through the nuclear pore complex is a multistep process. *J. Cell Biol.* 109:971–982.

Andrews, D. W., P. Walter, and F. P. Ottensmeyer. 1987. Evidence for an extended 7SL RNA structure in the signal recognition particle. *EMBO (Eur. Mol. Biol. Organ.) J.* 6:3471–3477.

Boublik, M., N. Robakis, W. Hellman, and J. S. Wall. 1982. Electron microscopic study of free ribosomes bound rRNA from E. coli. *Eur. J. Cell Biol.* 27:177–184.

Busch, H., R. Reddy, D. Henning, D. Spector, P. Epstein, N. Domae, M. Liu, S. Chirala, W. Schrier, and L. Rothblum. 1982. Gene Regulation. *UCLA Symp. Cell Mol. Biol.* 26:167–187.

Crowther, R. A., J. T. Finch, and B. M. F. Pearce. 1976. On the structure of coated vesicles. *J. Mol. Biol.* 103:785–798.

Dreyfuss, G. 1986. Structure and function of nuclear and cytoplasmic ribonucleoprotein particles. *Annu. Rev. Cell Biol.* 2:459–498.

Franke, W. W., U. Scheer, G. Krohne, and E.-D. Jarasch. 1981. The nuclear envelope and the architecture of the nuclear periphery. *J. Cell Biol.* 91:39s–50s.

Gall, J. G. 1967. Octagonal nuclear pores. *J. Cell Biol.* 32:391–399.

Gerace, L., Y. Ottaviano, and C. Kondor-Koch. 1982. Identification of a major polypeptide of the nuclear pore complex. *J. Cell Biol.* 95:826–837.

Hanover, J. A., C. K. Cohen, M. C. Willingham, and M. K. Park. 1987. O-linked N-acetylglucosamine is attached to proteins of the nuclear pore: evidence for cytoplasmic and nucleoplasmic glycoproteins. *J. Biol. Chem.* 262:9887–9894.

Heuser, J. 1980. Three-dimensional visualization of coated vesicle formation in fibroblasts. *J. Cell Biol.* 84:560–583.

Heuser, J. E. 1983. Procedure for freeze-drying molecules adsorbed to mica flakes. *J. Mol. Biol.* 169:155–195.

Heuser, J. E., and U. W. Goodenough. 1984. Structural comparison of purified dynein proteins with *in situ* dynein arms. *J. Mol. Biol.* 180:1083–1118.

Heuser, J. E., and T. Kirchausen. 1985. Deep-etch views of clathrin assemblies. *J. Ultrastruct. Res.* 92:1–27.

Holt, G. D., C. M. Snow, A. Senior, R. S. Haltwanger, L. Gerace, and G. W. Hart. 1987. Nuclear pore complex glycoproteins contain cytoplasmically disposed O-linked N-acetylglucosamine. *J. Cell Biol.* 104:1157–1164.

Kedersha, N. L., and L. H. Rome. 1986a. Isolation and characterization of a novel ribonucleoprotein particle: large structures contain a single species of small RNA. *J. Cell Biol.* 103:699–709.

Kedersha, N. L., and L. H. Rome. 1986b. Preparative agarose gel electrophoresis for the purification of small organelles and particles. *Anal. Biochem.* 156:161–170.

Kedersha, N. L., M.-C. Miquel, D. Bittner, and L. H. Rome. 1990. Vaults. II. Ribonucleoprotein structures are highly conserved among higher and lower eukaryotes. *J. Cell Biol.* 110:895–901.

Lake, J. A. 1978. Electron microscopy of specific proteins: three-dimensional mapping of ribosomal proteins using antibody labels. *In* Advanced Techniques in Biological Electron Microscopy II. J. K. Kohler, editors. Springer-Verlag, Berlin. 173–211.

Mandiyan, V., S. Tumminia, J. S. Wall, J. F. Hainfeld, and M. Boublik. 1989. Protein-induced conformational changes in 16S ribosomal RNA during the initial assembly steps of the Escherichia coli 30S ribosomal subunit. *J. Mol. Biol.* 210:323–336.

Mosesson, M. W., J. Hainfeld, J. Wall, and R. H. Haschemeyer. 1981. Identification and mass analysis of human fibrinogen molecules and their domains by scanning transmission electron microscopy. *J. Mol. Biol.* 153:695–718.

Nierhaus, K. H., R. Brimacomb, V. Nowotny, C. L. Pon, H. J. Rheinberger, B. Wittmann-Liebold, and H. G. Wittmann. 1987. New aspects of structure, assembly, evolution, and function of ribosomes. *Cold Spring Harbor Symp. Quant. Biol.* 52:665–674.

Olson, N. H., and T. S. Baker. 1989. Magnification calibration and the determination of spherical virus diameters using cryoelectron microscopy. *Ultramicroscopy.* 30:281–298.

Pardee, J. D., and J. A. Spudich. 1982. Purification of muscle actin. *Methods Enzymol.* 85:164–181.

Prasad, K., A. Alfsen, R. E. Lippoldt, P. K. Nandi, and H. Edelhoch. 1984. Structural characterization of labeled clathrin and coated vesicles. *Arch. Biochem. Biophys.* 238:403–410.

Reed, R., J. Griffith, and T. Maniatis. 1988. Purification and visualization of native spliceosomes. *Cell.* 53:949–961.

Reichelt, R., A. Holzenburg, E. L. Buhle, M. Jarnik, A. Engel, and U. Aebi. 1990. Correlation between structure and mass distribution of the nuclear pore complex and of distinct pore complex components. *J. Cell Biol.* 110:883–894.

Siegel, V., and P. Walter. 1988. Each of the activities of signal recognition particle (SRP) is contained within a distinct domain: analysis of biochemical mutants of SRP. *Cell.* 52:39–49.

Snow, C. M., A. Senior, and L. Gerace. 1987. Monoclonal antibodies identify a group of nuclear pore complex glycoproteins. *J. Cell Biol.* 104:1143–1156.

Steven, A. C., J. F. Hainfeld, J. S. Wall, and C. J. Steer. 1983. Mass distributions of coated vesicles isolated from liver and brain: analysis by scanning transmission electron microscopy. *J. Cell Biol.* 97:1714–1723.

Unwin, P. N. T., and R. A. Milligan. 1982. A large particle associated with the perimeter of the nuclear pore complex. *J. Cell Biol.* 93:63–75.

Vigers, G. P. A., R. A. Crowther, and B. M. F. Pearce. 1986. Three-dimensional structure of clathrin cages in ice. *EMBO (Eur. Mol. Biol. Organ.) J.* 5:529–534.

Walter, P., and G. Blobel. 1983. Disassembly and reassembly of signal recognition particle. *Cell.* 34:525–533.

Wittmann, H. G. 1983. Architecture of prokaryotic ribosomes. *Annu. Rev. Biochem.* 52:35–65.